Bond-length dependence of charge-transfer excitations and stretch phonon modes in perovskite ruthenates: Evidence of strong $p-d$ hybridization effects

J. S. Lee, Y. S. Lee, and T. W. Noh
School of Physics and Research Center for Oxide Electronics, Seoul National University, Seoul 151-747, Korea

S. Nakatsuji, H. Fukazawa, R. S. Perry, and Y. Maeno
Department of Physics, Kyoto University, Kyoto 606-8502, Japan

Y. Yoshida and S. I. Ikeda
National Institute of Advanced Industrial Science and Technology, Nanoelectronics Research Institute, Tsukuba, Ibaraki 305-8568, Japan

Jaejun Yu
School of Physics and Center for Strongly Correlated Materials Research, Seoul National University, Seoul 151-747, Korea

C. B. Eom
Department of Materials Science and Engineering, University of Wisconsin-Madison, Madison, Wisconsin 53706, USA
(Received 17 October 2003; revised manuscript received 12 March 2004; published 9 August 2004)

We reported the optical conductivity spectra of the Ruddlesden-Popper series ruthenates, i.e., $Sr_{n+1}Ru_nO_{3n+1}$ and $Ca_{n+1}Ru_nO_{3n+1}$, where $n=1$, 2, and ∞. Among various optical transitions, we investigated two Ru-O related modes, i.e., the charge-transfer excitation and the transverse stretching phonon. We found that their frequency shifts are not much affected by a structural dimensionality, but are closely related to the Ru-O bond length. Through the quantitative analysis of the charge-transfer excitation energy, we could demonstrate that the $p-d$ hybridization should play an important role in determining their electronic structure. In addition, we discussed how the electronic excitation could contribute the lattice dynamics in the metallic ruthenates.

DOI: 10.1103/PhysRevB.70.085103 PACS number(s): 78.20.−e, 78.30.−j, 78.40.−q

I. INTRODUCTION

Transition metal oxides are an intriguing material system where bondings between the outer most electron orbitals have both ionic and covalent characters. When the ionic character is dominant, then the long-range Coulomb interactions, called the Madelung potential, should play an important role and the correlation between electrons should be very strong. When the covalent character is dominant, the hybridization effects between O $2p$ and metal ion d orbitals, the so-called $p-d$ hybridization effects, should play a major role. Since both characters are comparable in transition metal oxides, their physical properties have been difficult to understand either from the localized ionic picture or from the band picture, and have been important topics in condensed matter physics.

Optical spectroscopy has been proven to be a useful method to investigate the bonding natures in the strongly correlated electron systems. In cuprates, many workers systematically investigated charge-transfer optical excitations, i.e., optical transitions between the O $2p$ states and the Cu $3d$ states,[1–5] and could successfully understand the nature of the bonding character between the $2p$ states and the $3d$ states. They found that the trend in the charge-transfer excitations could be explained mainly by variation of the Madelung potential, suggesting that the O $2p$-Cu $3d$ bondings could have a strong ionic character. Similar observations have been made for other $3d$ transition metal oxides, such as nickelates.[6]

Through the extensive investigations on ruthenates, after the discovery of the unconventional superconductivity in Sr_2RuO_4,[7] we have accumulated a large understanding of the $4d$ transition metal oxides.[8–12] Numerous intriguing physical phenomena, including metal-insulator transition and superconductivity, have been observed in the ruthenates, and explained in terms of electron-electron interactions.[12–14] However, due to their more extended $4d$ orbitals, ruthenates should have weaker electron-electron interaction but stronger $p-d$ hybridization effects than those of the $3d$ transition metal oxides. In the perovskite ruthenates, a distortion in the RuO_6 networks results in a weakening of the π overlap between the oxygen p and the Ru t_{2g} orbitals. Such electron-lattice interactions, which are strongly coupled with the $p-d$ hybridization, can be greatly enhanced due to the extended character of the $4d$ orbitals. Actually, both LSDA electronic structure calculations and the photoemission spectroscopy study for $SrRuO_3$ revealed that the electronic structure shows a strong $2p-4d$ hybridization throughout the whole valence-band and conduction-band regions.[14,15]

In this paper, we investigated the bonding nature of the O $2p$ and Ru $4d$ orbitals by calculating the Madelung potentials and analyzing optical conductivity spectra $\sigma(\omega)$ of the Ruddlesden-Popper (RP) series $(Sr,Ca)_{n+1}Ru_nO_{3n+1}$ ($n=1$, 2, and ∞). In these ruthenates, the valency of the Ru ions remains the same, i.e., 4+, but their structural parameters, such as dimensionality, bond length, and bond angle, exhibit systematic variations.[16–20] Note that the Madelung potential will

 ©2004 The American Physical Society

be determined how the ions are arranged, so it should be strongly dependent on the system dimensionality. Therefore, $(Sr,Ca)_{n+1}Ru_nO_{3n+1}$ could be an ideal material system to determine which structural parameters are crucial to determine the electronic structures of ruthenates: If the dimensionality becomes important, then the bonds should have a strong ionic character, but if the other structural parameters become important, then the covalent characters should be more important.

II. EXPERIMENTAL TECHNIQUES

Single crystals of Sr_2RuO_4 (Sr214), Ca_2RuO_4 (Ca214), $Sr_3Ru_2O_7$ (Sr327), and $Ca_3Ru_2O_7$ (Ca327) were grown by the floating zone method.[21–23] High-quality $SrRuO_3$ (Sr113) and $CaRuO_3$ (Ca113) films were epitaxially grown with the *c*-axis orientation on a $SrTiO_3$ substrate using the pulsed laser deposition and sputtering techniques, respectively.[24,25] The film thicknesses were larger than 4000 Å. Near-normal incidence reflectivity spectra of the *ab* plane were measured between 5 meV and 30 eV. Below 0.8 eV, a Fourier transform spectrophotometer was used. Between 0.6 and 6.0 eV, grating spectrometers were used. Above 6.0 eV, the synchrotron radiation at Pohang Light Source (PLS) was used. Using the Kramers-Kronig analysis, $\sigma(\omega)$ were obtained. The details of the reflectivity measurements and the Kramers-Kronig analysis were given elsewhere.[26]

III. RESULTS AND DISCUSSIONS

A. The Ru-O interband transition

Figures 1(a) and 1(b) show the room temperature $\sigma(\omega)$ of $Sr_{n+1}Ru_nO_{3n+1}$ and $Ca_{n+1}Ru_nO_{3n+1}$, respectively. Both of the figures show that the spectral features are mainly composed of two parts: namely, the Drude-like peak centered at the zero frequency and interband transitions above 1 eV. The coherent Drude-like peaks were observed for all the samples except Ca214. The existence of the coherent peaks indicates that they should be in metallic states, consistent with their dc-transport results.[7,8,18,27] For Ca214, an optical gap can be clearly seen, revealing its insulating character. The sharp spikes in the far-infrared region come from absorptions by the transverse optical phonon modes.

Among the interband transitions, we pay attention to the strong peaks just above 3.0 eV, which are observed in all of the spectra. The peaks correspond to the interband transitions between the O 2*p* band and the Ru t_{2g} band,[11,12,28] so their energy positions should be directly related to the charge-transfer energy Δ_{p-d}, i.e., the energy difference between two bands. Using the fitting of $\sigma(\omega)$ with the Lorentz oscillators, we were able to obtain Δ_{p-d}. The second row of Table I shows the values of Δ_{p-d}, estimated by assuming that the strong peak feature around 3.0 eV could be fitted with a single Lorentz oscillator. Since such absorption features for Sr214 and Sr327 are rather broad, we could also fit them with two Lorentz oscillators. [The inset of Fig. 1(a) shows the fitting result for Sr214 with two Lorentz oscillators.] And, Δ_{p-d} could be estimated as the midpoints of the peaks, which are nearly the same as those of Table I.[29] With increasing *n*, Δ_{p-d} for the Sr series decreases systematically by about 0.9 eV, but that for the Ca series shows little change.

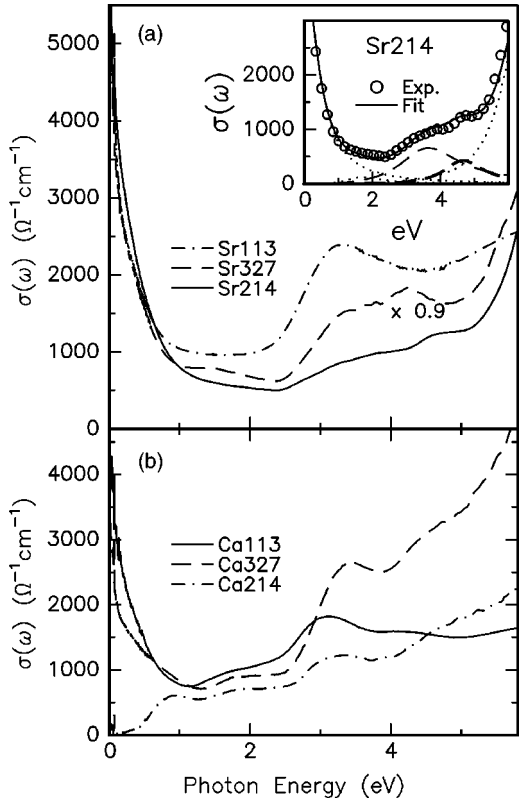

FIG. 1. The room-temperature optical conductivity spectra $\sigma(\omega)$ of (a) $SrRuO_3$ (Sr113), $Sr_3Ru_2O_7$ (Sr327), and Sr_2RuO_4 (Sr214), and (b) $CaRuO_3$ (Ca113), $Ca_3Ru_2O_7$ (Ca327), and Ca_2RuO_4 (Ca214). The inset of (a) shows a fitting result for Sr214 using the Lorentz oscillators. The spectral shape of a coherent peak is fitted with a truncated Lorentzian. And, the peak just above 3 eV is assumed to be composed of two peaks around 3.65 and 4.7 eV.

For cuprates and nickelates,[2–6] it was already known that the dimensionality, which is related to the coordination number of the oxygen atoms for the transition metal ion, should play an important role. To check this possibility, we plotted the dimensionality dependences of the Δ_{p-d} values in Fig. 2(a). Here, we adopt the value of $(3-1/n)$ as a dimensional parameter. Then, $n=1$, 2, and ∞ correspond to the two, 2.5, and three-dimensional cases, respectively. As dimensionality (or *n*) increases, Δ_{p-d} for the Sr series (the closed circles) shifts significantly to the lower energy. On the other hand, for the Ca series (the closed triangles), Δ_{p-d} does not show such systematic trends, but remains at nearly the same energy. These differences demonstrate that the variation of Δ_{p-d} in these perovskite ruthenates could not be explained with only the consideration of the structural dimensionality.

For a more quantitative argument, we calculated the energy levels based on a simple ionic model, where the Madelung potential should be varied for different ionic arrangements, and depend on the dimensionality. Note that Δ_{p-d} corresponds to the energy cost to excite an electron from an O^{2-} ion to a neighboring metal Ru^{4+} ion. This involves the difference between the ionization potential $I(O^{2-})$ of the O^{2-} ion and the electron affinity $A[=I(Ru^{4+})]$ of the Ru^{4+} ion. In

TABLE I. Values of the charge-transfer energy Δ_{p-d}, the Madelung potential $e\Delta'_{Mad}$, the Ru-O bond length d_{Ru-O}, the corresponding bond angle θ, and the transverse optical phonon frequency ω_{TO} of the perovskite ruthenates. (Note that values of $e\Delta'_{Mad}$ were calculated Madelung potential differences relative to the Sr214 value.)

	Sr series			Ca series		
	Sr214	Sr327	Sr113	Ca214	Ca327	Ca113
Δ_{p-d}(eV)	4.15	3.78	3.28	3.25	3.35	3.08
$e\Delta V'_{Mad}$(eV)	0	−0.16	−0.32	−0.11	−0.14	−0.31
d_{Ru-O}(Å)	1.935[a]	1.957[b]	1.983[c]	1.990[a]	1.994[d]	1.991[c]
θ(°)	180[a]	168[b]	165[c]	154[a]	150[d]	150[c]
ω_{TO}(cm^{-1})	670	619	581	584	575	569

[a]Reference 16.
[b]Reference 17.
[c]Reference 18 and 19.
[d]Reference 20.

addition, there exists a term ΔV_{Mad}, i.e., the difference in the electrostatic Madelung site potentials of the Ru^{4+} and the O^{2-} ions. Consequently,

$$\Delta_{p-d} \equiv A(O^-) - I(\mathrm{Ru}^{4+}) + e\Delta V_{Mad} - e^2/d_{Ru\text{-}O}, \qquad (1)$$

where the term e^2/d_{M-O} includes the Coulomb interaction from the electron and hole pair, the so-called exciton, formed by the optical absorption. In Eq. (1), $A(O^-) - I(Ru^{4+})$ should be the same for all of the ruthenates studied since it is the value of the level separation between the O^{2-} and Ru^{4+} ions in the atomic limit. Also, the variation of the excitonic energy contributions is at most 0.1 eV, which is smaller than the variation of $e\Delta V_{Mad}$. So, in this simple ionic picture, Δ_{p-d} should be mainly determined by $e\Delta V_{Mad}$. Taking into account all of the structural information, including the dimensionality and the structural distortion,[16–20] we calculated the Madelung site potential based on a full-potential electronic structure. The third row of Table I shows the values of $e\Delta V'_{Mad}$ [$\equiv e\Delta V_{Mad} - e\Delta V_{Mad}$(Sr214)], which is the ΔV_{Mad} value difference with respect to the corresponding Sr214 value.

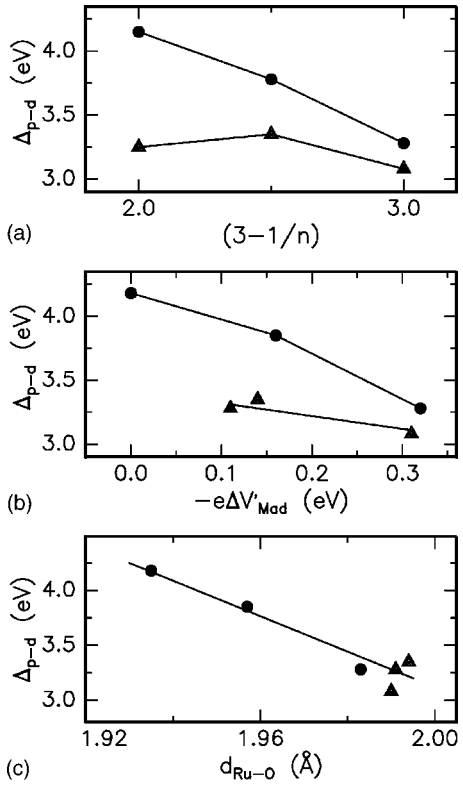

FIG. 2. The dependences of Δ_{p-d} (a) on the dimensional parameter $(3-1/n)$, (b) on the Madelung potential difference $-e\Delta V'_{Mad}$, and (c) on the Ru-O bond length d_{Ru-O}. The solid lines are guides for the eye. The data for the Sr and the Ca series are shown as closed circles and triangles, respectively.

The simple ionic model has proven useful for calculating the electronic state of oxides which have rather strongly localized electrons. In addition, based on the ionic model, Torrance *et al.* calculated the parameters of the Coulomb repulsion energy and the charge-transfer energy, and categorized numerous 3*d* and 4*d* transition metal compounds into two groups, i.e., metals and insulators, on the basis of the Zaanen-Sawatzky-Allen scheme, and found that they are consistent with their actual ground states.[30] Therefore, we think that it can be a good starting point to understand the electronic states of the metallic ruthenates, which also have been considered as a strongly correlated electron system.[12,14]

Figure 2(b) shows the dependence of Δ_{p-d} on $-e\Delta V'_{Mad}$. [Note that Figs. 2(a) and 2(b) are similar to each other, which indicates that the $e\Delta V'_{Mad}$ values are closely related to the structural dimensionality.] If the simple ionic model is valid, all of the data, including those for the Sr and the Ca series, should fall on a single straight line. When we look at just the data for the Ca series, the change of Δ_{p-d} seems to be in reasonably good agreement with $e\Delta V'_{Mad}$. For the Sr series, although their Δ_{p-d} values also seem to be linearly increasing with $e\Delta V'_{Mad}$, their values are much larger than those for the Ca series. Moreover, its slope is also larger than that of the Ca series. If existent, the Madelung potential contribution (i.e., the ionic bond character) should not be large enough to explain the systematic variation of the 3.0 eV interband transition, at least for the Sr series.

Now, let us look into the dependence of Δ_{p-d} on in-plane bond length between the Ru and the O ions, d_{Ru-O}. (For the

113 compounds, d_{Ru-O} corresponds to the average bond length.[19,20]) As can be seen from the second and fourth rows of Table I, Δ_{p-d} decreases drastically with the increase of d_{Ru-O}.[16–18] Figure 2(c) shows a plot of Δ_{p-d} vs d_{Ru-O}. Note that all of the experimental data from the Sr and the Ca series fall on a single line. An analysis based on pseudopotential theory predicts that the hybridization strength t should be proportional to $1/d_{Ru-O}^{3.5}$ (Ref. 31). This gives rise to an additional energy separation between the states with the main character of the p and d orbitals, proportional to t^2/Δ_{p-d}.[1,32] In these respects, the strong d_{Ru-O} dependence of Δ_{p-d} demonstrates that the short-range contribution specified by a bond length should be of significance, and the $p-d$ hybridization effect plays an important role in determining the electronic structure of these ruthenates.[33]

It would be interesting to compare our results with those of other transition metal oxides. For cuprates, while the charge-transfer energy is partly determined by the Cu-O bond length,[1] it is also strongly influenced by the coordination number of the system or by the system dimensionality.[2–4] Ohta *et al.* have demonstrated that a fairly large variation of Δ_{p-d} in insulating cuprates could be well explained by ΔV_{Mad}.[5] For nickelates also, the change of the Madelung potential, related to the structural dimensionality, could explain the large variations of the charge-transfer energies.[6] On the other hand, for ruthenates, while the charge-transfer energy is not much influenced by the structural dimensionality, it is found to be closely related to the Ru-O bond length. Based on these comparisons, we could conclude that ruthenates should have stronger $p-d$ hybridization effects than cuprates and nickelates, which could originate from the extended character of the 4d orbitals.

One of the interesting puzzling behaviors in the perovskite ruthenates is that the dimensionality dependence of the electrical properties of the Sr series is different from that of the Ca series: namely, while the two-dimensional Sr214 is the most metallic in the Sr series, Ca214 is the most insulating in the Ca series. In most perovskites, as n increases, the metallicity also increases. The rather strong hybridization effects, discussed above, can provide a reasonable explanation. When the hybridization between the O $2p$ and the Ru t_{2g} bands becomes important, we have to consider the nearest-neighbor interaction, represented by a transfer integral proportional to $|\cos\theta|/d_{Ru-O}^{3.5}$ together with the dimensionality effects.[31] Here, θ is the Ru-O-Ru bond angle. As shown in Table I, while the Sr series exhibits quite significant variations for d_{Ru-O} and θ, three Ca series samples have nearly the same values. Consequently, for the Ca series the dimensionality effect is dominant, and the 2-dimensional Ca214 is the most insulating. However, for Sr214, which has the largest θ and the smallest d_{Ru-O}, the large transfer integral contributes its metallicity, and its effect should be much larger than the dimensionality contribution.

B. The Ru-O stretching phonon

Figure 3 shows the far-infrared $\sigma(\omega)$ of $Sr_{n+1}Ru_nO_{3n+1}$ and $Ca_{n+1}Ru_nO_{3n+1}$ between 500 and 750 cm^{-1}, respectively. All of the spectra show a peak due to the transverse in-plane

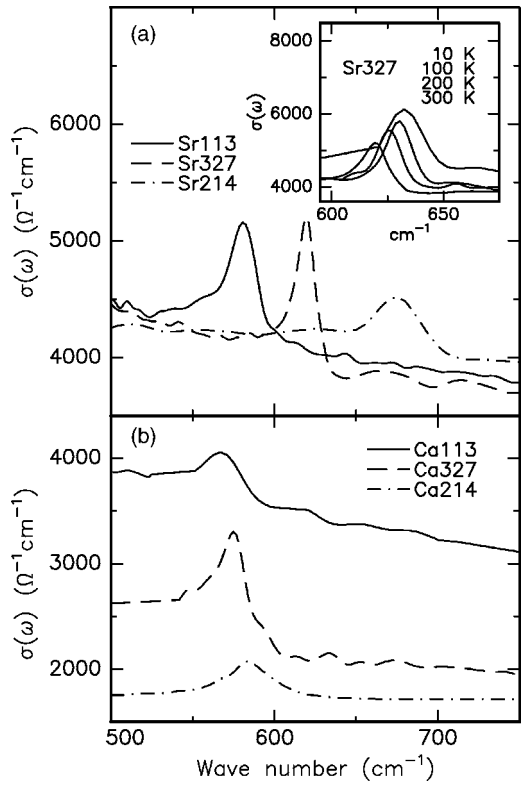

FIG. 3. The far-infrared optical conductivity spectra $\sigma(\omega)$ of (a) the perovskite Sr-ruthenate series, and (b) the perovskite Ca-ruthenate series. Since Ca214 is in the insulating state, its corresponding $\sigma(\omega)$ is low. So, its $\sigma(\omega)$ is plotted with an upward shift by 1200 Ω^{-1} cm^{-1}. The inset displays the temperature-dependent $\sigma(\omega)$ of the Sr327 sample.

Ru-O stretch phonon mode.[11] Since most of the samples are in metallic states, the phonon features are rather weak compared to the broad Drude background. The phonon frequency ω_{TO} for the Sr series exhibits a dramatic shift of around 100 cm^{-1} as n varies. However, ω_{TO} for the Ca series remains at nearly the same value. Note that these trends are quite similar to those of the 3.0 eV interband transitions, shown in Fig. 1. In addition, for Sr327, we measured the phonon spectra at various temperatures. As shown in the inset of Fig. 3, ω_{TO} of Sr327 increases by about 15 cm^{-1} as temperature decreases from 300 to 10 K.

It is well known that ω_{TO} will depend on the crystal structure, especially on the bond length d. When d increases, the restoring force of the vibration mode decreases, resulting in a decrease of ω_{TO}. In a simple model where neutral atoms are vibrating in a periodic harmonic potential, $\omega_{TO} \sim d^{-1.5}$ (Ref. 34). In Fig. 4(a), ω_{TO} is plotted in terms of d_{Ru-O}. To see the power dependence of ω_{TO} on d_{Ru-O}, we made a log-log plot. As d_{Ru-O} increases, ω_{TO} decreases. However, the decrease of ω_{TO} is much faster than $d^{-1.5}$, which is displayed as a dotted line. Actually, all of the Sr and the Ca series data, including the temperature-dependent Sr327 data, fall onto the solid line with a slope of −5.5, indicating that $\omega_{TO} \sim d_{Ru-O}^{-5.5}$ This strong dependence on d_{Ru-O} indicates that we should look for some interactions beyond a harmonic potential.

Similar strong d dependences of ω_{TO} have been also observed in the insulating cuprates and some manganites.[35–37]

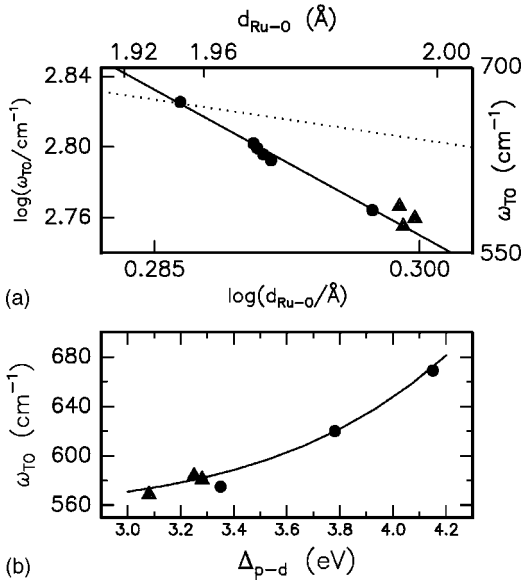

FIG. 4. (a) The dependence of ω_{TO} on d_{Ru-O}. The solid and the dotted lines represent $\omega_{TO} \propto d_{Ru-O}^{-5.5}$ and $\omega_{TO} \propto d_{Ru-O}^{-1.5}$, respectively. Temperature-dependent values for Sr327 are also shown at $\log(d_{Ru-O}) \sim 0.29$. (b) Dependence of ω_{TO} on Δ_{p-d}. The closed circles and triangles correspond to the data of the Sr and the Ca series, respectively.

These phenomena have been explained in terms of the so-called interband electron-phonon coupling. During the lattice vibration, the atomic displacements can be coupled to each other through the polarizations of valence electrons. From a band-view point, such interband polarization of valence electrons can be induced by the interband electron-TO phonon coupling.[38] Figure 4(b) shows the plot of ω_{TO} vs Δ_{p-d}, which shows a monotonic increase of ω_{TO} as Δ_{p-d} increases, for all of ruthenates. This indicates a possible coupling of the Ru-O stretching phonon mode with the Ru-O charge-transfer electronic excitation, which should originate from the strong $p-d$ hybridization. Note that, in cuprates and some manganites, the strong d dependences of ω_{TO} were only observed for the insulating (or semiconducting) states. However, in our ruthenates, the strong dependence of ω_{TO} on d_{Ru-O} was observed for mostly metallic states. The extended nature of the $4d$ orbitals in the ruthenates could result in the strong d_{Ru-O} dependence of ω_{TO}, even in the metallic states through the strong $p-d$ hybridization. More systematic studies are desirable in order to elucidate the interband electron-phonon coupling.

IV. SUMMARY

We reported the optical conductivity spectra of the Ruddlesden-Popper series ruthenates $(Sr,Ca)_{n+1}Ru_nO_{3n+1}$ ($n=1$, 2, and ∞). As dimensionality (or n) varies and/or the Ca ion is substituted by the Sr ion, there are unusual peak shifts in two Ru-O related modes, i.e., the Ru-O interatomic charge-transfer excitation and the Ru-O transverse stretch phonon mode. In order to obtain a proper understanding, we should consider short-range contributions, specified by bond length, rather than the long-range contributions, such as the Madelung potential. The importance of the short-range contributions suggests that the $p-d$ hybridization should play an important role in determining the electronic structures and the lattice dynamics of the perovskite ruthenates.

ACKNOWLEDGMENTS

We would like to thank Yunkyu Bang for helpful discussions. This work was supported by the Ministry of Science and Technology through the Creative Research Initiative program, and by KOSEF through the Center for Strongly Correlated Materials Research. The experiments at PLS were supported by MOST and POSCO.

[1] S. L. Cooper, G. A. Thomas, A. J. Millis, P. E. Sulewski, J. Orenstein, D. H. Rapkine, S-W. Cheong, and P. L. Trevor, Phys. Rev. B **42**, 10 785 (1990).
[2] Y. Tokura, K. Kikuchi, T. Arima, and S. Uchida, Phys. Rev. B **45**, 7580 (1992).
[3] T. Arima, K. Kikuchi, M. Kasuya, S. Koshihara, Y. Tokura, T. Ido, and S. Uchida, Phys. Rev. B **44**, 917 (1991).
[4] Y. Tokura, S. Koshihara, T. Arima, H. Takagi, S. Ishibashi, T. Ido, and S. Uchida, Phys. Rev. B **41**, 11 657 (1990).
[5] Y. Ohta, T. Tohyama, and S. Maekawa, Phys. Rev. Lett. **66**, 1228 (1991), and references therein.
[6] K. Maiti, Priya Mahadevan, and D. D. Sarma, Phys. Rev. B **59**, 12 457 (1999).
[7] Y. Maeno, H. Hashimoto, K. Yoshida, S. Nishizaki, T. Fujita, J. G. Bednorz, and F. Lichtenberg, Nature (London) **372**, 532 (1995).
[8] S. Nakatsuji and Y. Maeno, Phys. Rev. Lett. **84**, 2666 (2000).
[9] S. A. Grigera, R. S. Perry, A. J. Schofield, M. Chiao, S. R. Julian, G. G. Lonzarich, S. I. Ikeda, Y. Maeno, A. J. Millis, and A. P. Mackenzie, Science **294**, 329 (2001).
[10] Y. S. Lee, J. S. Lee, K. W. Kim, T. W. Noh, Jaejun Yu, E. J. Choi, G. Cao, and J. E. Crow, Europhys. Lett. **55**, 280 (2001); Y. S. Lee, J. S. Lee, T. W. Noh, D. Y. Byun, K. S. Yoo, K. Yamaura, and E. Takayama-Muromachi, Phys. Rev. B **67**, 113101 (2003).
[11] J. S. Lee, Y. S. Lee, T. W. Noh, S.-J. Oh, Jaejun Yu, S. Nakatsuji, H. Fukazawa, and Y. Maeno, Phys. Rev. Lett. **89**, 257402 (2002).
[12] J. S. Lee, Y. S. Lee, T. W. Noh, K. Char, Jonghyurk Park, S.-J. Oh, J.-H. Park, C. B. Eom, T. Takeda, and R. Kanno, Phys. Rev. B **64**, 245107 (2001).
[13] Y. S. Lee, J. S. Lee, T. W. Noh, T. H. Gimm, H. Y. Choi, J. Yu, and C. B. Eom, Phys. Rev. B **66**, 041104 (2003).
[14] J. Okamoto, T. Mizokawa, and A. Fujimori, Phys. Rev. B **60**, 2281 (1999).

[15] D. Singh, J. Appl. Phys. **79**, 4818 (1996).
[16] O. Friedt, M. Braden, G. Andre, P. Adelmann, S. Nakatsuji, and Y. Maeno, Phys. Rev. B **63**, 174432 (2001).
[17] H. Shaked, J. D. Jorgensen, S. Short, O. Chmaissem, S.-I. Ikeda, and Y. Maeno, Phys. Rev. B **62**, 8725 (2000).
[18] G. Cao, K. Abboud, S. McCall, J. E. Crow, and R. P. Guertin, Phys. Rev. B **62**, 998 (2000).
[19] Q. Gan, R. A. Rao, C. B. Eom, J. L. Garrett, and M. Lee, Appl. Phys. Lett. **72**, 978 (1998).
[20] H. Kobayashi, M. Nagata, R. Kanno, and Y. Kawamoto, Mater. Res. Bull. **29**, 1271 (1994).
[21] S. Nakatsuji and Y. Maeno, J. Solid State Chem. **156**, 26 (2001).
[22] S. I. Ikeda and Y. Maeno, Physica B **259-261**, 947 (1999).
[23] Y. Yoshida, S. I. Ikeda, I. Nagai, and N. Shirakawa, J. Low Temp. Phys. **131**, 1135 (2003).
[24] L. Mieville, T. H. Geballe, L. Antognazza, and K. Char, Appl. Phys. Lett. **70**, 126 (1997).
[25] R. A. Rao, Q. Gan, C. B. Eom, R. J. Cava, Y. Suzuki, J. J. Krajewski, S. C. Gausepohl, and M. Lee, Appl. Phys. Lett. **70**, 3035 (1997).
[26] H. J. Lee, J. H. Jung, Y. S. Lee, J. S. Ahn, T. W. Noh, K. H. Kim, and S.-W. Cheong, Phys. Rev. B **60**, 5251 (1999).
[27] S. I. Ikeda, Y. Maeno, S. Nakatsuji, M. Kosaka, and Y. Uwatoko, Phys. Rev. B **62**, R6089 (2000).
[28] J. S. Dodge, E. Kulatov, L. Klein, C. H. Ahn, J. W. Reiner, L. Mieville, T. H. Geballe, M. R. Beasley, A. Kapitulnik, H. Ohta, Yu. Uspenskii, and S. Halilov, Phys. Rev. B **60**, R6987 (1999).
[29] As a two-peak structure is assumed for the $p-d$ transition of Sr214 and Sr327, Δ_{p-d} could also be estimated as the positions of the lower energy peaks which were found to be somewhat smaller than the Δ_{p-d} value in Table I. Even if the estimated lower energy peak positions were used for Δ_{p-d}, most of the conclusions based on the single Lorentz oscillator are still valid.
[30] J. B. Torrance, P. Lacorre, C. Asavaroengchai, and R. M. Metzgar, Physica C **182**, 351 (1991).
[31] W. A. Harrison, *Electronic Structure and Physical Properties of Solids* (Freeman, San Francisco, 1980).
[32] M. Imada, A. Fujimori, and Y. Tokura, Rev. Mod. Phys. **70**, 1039 (1998), and references therein.
[33] In the Sr series, the $p-d$ transition becomes very broad with decreasing n. The two-dimensionality and the elongation of RuO_6 octahedra of the layered ruthenates will give rise to the different $p-d$ hybridization strengths of the d_{xy} and d_{yz}/d_{zx} orbitals.[16] The $p-d$ transitions related with each hybridized d orbital state could therefore have different energy levels. Consequently, the very broad charge-transfer excitations of Sr214 and Sr327 can also be considered as a result of the strong $p-d$ hybridization.
[34] A. de Andres, S. Taboada, J. L. Martinez, A. Salinas, J. Hernandez, and R. Saez-Puche, Phys. Rev. B **47**, 14 898 (1993).
[35] S. Tajima, T. Ido, S. Ishibashi, T. Itoh, H. Eisaki, Y. Mizuo, T. Arima, H. Takagi, and S. Uchida, Phys. Rev. B **43**, 10 496 (1991).
[36] A. de Andres, S. Taboada, J. L. Martinez, A. Salinas, J. Hernandez, and R. Saez-Puche, Phys. Rev. B **47**, 14 898 (1993).
[37] A. V. Boris, N. N. Kovaleva, A. V. Bazhenov, A. V. Samoilov, N.-C. Yeh, and R. P. Vasquez, J. Appl. Phys. **81**, 15 (1997).
[38] H. Kawamura, S. Katayama, S. Takano, and S. Hotta, Solid State Commun. **14**, 259 (1974); S. Katayama and H. Kawamura, *ibid.* **21**, 521 (1977).